Ghignone *et al. Swiss J Geosci* (2020) 113:17
https://doi.org/10.1186/s00015-020-00370-6

SGG SGS sc | nat
Swiss Journal of Geosciences

ORIGINAL PAPER Open Access

Structural evolution along the Susa Shear Zone: the role of a first-order shear zone in the exhumation of meta-ophiolite units (Western Alps)

Stefano Ghignone*, Gianni Balestro, Marco Gattiglio and Alessandro Borghi

Abstract

In the Western Alps, different shear zones acting at different depths have been investigated for explaining multistage exhumation of (U)HP units, and several exhumation models have been proposed for explaining present-day stacking of different tectonometamorphic units. This study aims to reconstruct the tectonic evolution of the Susa Shear Zone (SSZ), a polyphasic first-order shear zone, outcropping in the Susa Valley. The SSZ consists of a thick mylonitic zone, along which units characterized by different Alpine metamorphic P–T peaks are coupled. In the study area, the footwall of the SSZ mostly consists of oceanic units (i.e., Internal Piedmont Zone), which record eclogitic conditions, whereas the hanging wall consists of oceanic units (i.e., External Piedmont Zone), which record blueschist-facies conditions. These tectonic units were deformed during subduction- and exhumation-related Alpine history, throughout four main regional deformation phases (from D1 to D4), and were coupled along the SSZ, wherein two shearing events have been distinguished (T1 and T2). T1 occurred during early exhumation and was characterized by "apparent reverse" Top-to-E kinematics, whereas T2 occurred during late exhumation and was characterized by Top-to-W kinematics. Detailed fieldwork and structural analysis allowed us to describe the main features of the different deformation stages and define the deformation relative timing. As final result, we propose a four-step geodynamic model, focused on the different stages developed along the SSZ, from pre-T1 to syn-T2, showing the geometrical relationships between the tectonic units involved in the exhumation. The model aims at explaining the role of the SSZ in the axial sector of the Western Alps.

Keywords: Western Alps, Structural evolution, Susa valley, Susa Shear Zone, Exhumation

1 Introduction

Understanding the building of collisional orogenic belts, and related subduction and exhumation processes, is a much-debated topic. The reconstruction of various evolution stages, recorded by tectonic units during their paths into the orogenic wedge, provides precise information about architecture and geodynamic of orogenic belts. In the Western Alps, several models have been proposed (see e.g., Butler et al. 2013) to explain the present-day stacking order of crustal units. The study of terranes coupled during exhumation focused on first-order shear zones that shaped the nappe stack and wherein polyphasic kinematics are recorded. Different Alpine shear zones acting at different depths have been investigated for explaining exhumation of (U)HP units in the axial sector of the Western Alps (see Platt 1993; Kurz and Froitzheim 2002 as reviews).

In this study, the polyphasic tectonic evolution of a first-order shear zone (i.e., the Susa Shear Zone, SSZ; see

Editorial handling: Paola Manzotti

*Correspondence: s.ghignone@unito.it
Dipartimento Di Scienze Della Terra, Università Degli Studi Di Torino, Via Valperga Caluso, 35, 10125 Torino, Italy

Ghignone et al. 2020a and references therein), outcropping in the inner sector of the Western Alps, is presented. The SSZ is a thick mylonitic zone, along which different shearing events occurred. Oceanic units are coupled along the SSZ, belonging to the Internal Piedmont Zone (IPZ hereafter) in the footwall, and to the External Piedmont Zone (EPZ hereafter) in the hanging wall.

The two units are characterized by different Alpine metamorphic P–T peaks: the footwall units record eclogite-facies conditions, whereas the hanging wall units record blueschist-facies conditions. The metamorphic jump in P between the two units is about 10 kbar: ~10–12 kbar between Zermatt-Saas (P = 25–30 kbar, T = 550–600 °C, Bucher et al. 2005; Angiboust et al. 2009) and Combin (P = 12–13 kbar, T = 425–475 °C, Cartwright and Barnicoat 2002; Negro et al. 2013) units, ~10 kbar between Monviso (roughly P = 25 kbar and T = 550 °C, Balestro et al. 2014; Groppo and Castelli 2010) and Queyras (P = 8–14 kbar, T = 300–475 °C, Michard et al. 2003; Tricart and Schwartz 2006) units. In the study area, the metamorphic jump in P between the IPZ and EPZ is >5 kbar (Agard et al. 2001, 2002; Angiboust and Glodny 2020; Ghignone et al. 2020b).

The occurrence of (i) polyphasic kinematic indicators and of (ii) a metamorphic jump from the eclogite-facies footwall to the blueschist-facies hanging wall, are the main characteristics of the SSZ. Similar features were reported in other sectors of the Western Alpine axial belt, as described by Phillipot (1990), and Ballèvre et al. (1990) (i.e., the West Viso Detachment), and by Ballèvre and Merle (1993), and Pleuger et al. (2007) (i.e., the Combin Fault). These shear zones can be considered the southern and northern equivalents of the SSZ (Ghignone et al. 2020a).

Through detailed fieldwork, geological mapping and structural analysis, we describe here the tectonic evolution that occurred along the SSZ. We detected distinct stages in the evolution of the SSZ and of its footwall and hanging wall blocks, disclosing some key steps of the building of this sector of the Western Alpine belt.

2 Regional geology

The Western Alps (Fig. 1) are a collisional belt that originated from convergence between the Adria upper plate and the European lower plate, and the interposed Alpine Tethys, which developed during Middle to Late Jurassic spreading of oceanic crust (Lemoine and Tricart 1986; Michard et al. 1996; Vissers et al. 2013; Balestro et al. 2019). The axial sector of the Western Alpine belt, consisting of the most deformed (U)HP tectono-metamorphic units, corresponds to an exhumed fossil subduction-complex, which was overthrusted on the European and Adriatic forelands to the NW and to the SE, respectively (Ricou and Siddans 1986; Rosenbaum and Lister 2005; Schmid et al. 2017). The present-day architecture of the axial sector resulted from three main tectonic stages developed during the (i) Late Cretaceous to Middle Eocene subduction and HP metamorphism, (ii) Late Eocene to Early Oligocene collision-related NW-verging accretion and metamorphic re-equilibration, and (iii) Late Oligocene to Neogene deep Adriatic crust/mantle indentation and shallow crustal tectonic (e.g., Le Bayon and Ballèvre 2006; Lardeaux et al. 2006; Manzotti et al. 2014; Balestro et al. 2015b; Festa et al. 2020).

Remnants of the Alpine Tethys (i.e., the Piedmont Zone; see e.g., Martin et al. 1994), were tectonically sandwiched between the overlying Adriatic continental margin units and the underlying European ones (Dal Piaz et al. 2003 and references therein). Based on different tectonic position, metamorphic evolution and lithostratigraphy, meta-ophiolite units of the Western Alps have been historically distinguished into Internal Piedmont Zone (IPZ) and External Piedmont Zone (EPZ), i.e., Zermatt-Saas-like units and Combin-like units of Bearth (1967), respectively. The IPZ was metamorphosed under eclogite-facies P–T peak conditions and consists of meta-ophiolite covered by thin metasedimentary successions (see e.g., Balestro et al. 2014, 2018; Tartarotti et al. 2017, and references therein), whereas the EPZ was metamorphosed under blueschist-facies P–T peak conditions, and consist of meta-ophiolite bodies scattered within thick metasedimentary successions (see e.g., Agard et al. 2001; Schwartz et al. 2009).

The IPZ units tectonically overly the Internal Crystalline Massifs (ICM: Monte Rosa, MR, Gran Paradiso, GP, and Dora-Maira, DM; see e.g., Gasco et al. 2013 and references therein). These massifs consist of composite polymetamorphic basements intruded by post-Variscan metagranite and metadiorite bodies, and covered by discontinuous Permian metavolcanic rocks, Permian to Early Triassic siliciclastic metasediments and Middle to Late Triassic carbonate metasediments. The ICM and IPZ units record an Alpine metamorphic evolution characterized by a first main eclogite-facies stage, usually regarded as Eocene (see e.g., Rosenbaum and Lister 2005; Weber et al. 2015 and references therein), and a low-P greenschist to amphibolite facies re-equilibration of Upper Eocene to Lower Oligocene age (see Beltrando et al. 2010; Gauthiez-Putallaz et al. 2016; Manzotti et al. 2018). The EPZ units tectonically lie above both the IPZ and Middle Penninic units, which were metamorphosed under blueschist-facies P–T peaks conditions (Ganne et al. 2003, 2006, 2007). The Middle Penninic units consist of composite polymetamorphic basements, post-Variscan meta-intrusives, widespread Carboniferous to Permian metasediments and thick Mesozoic carbonate

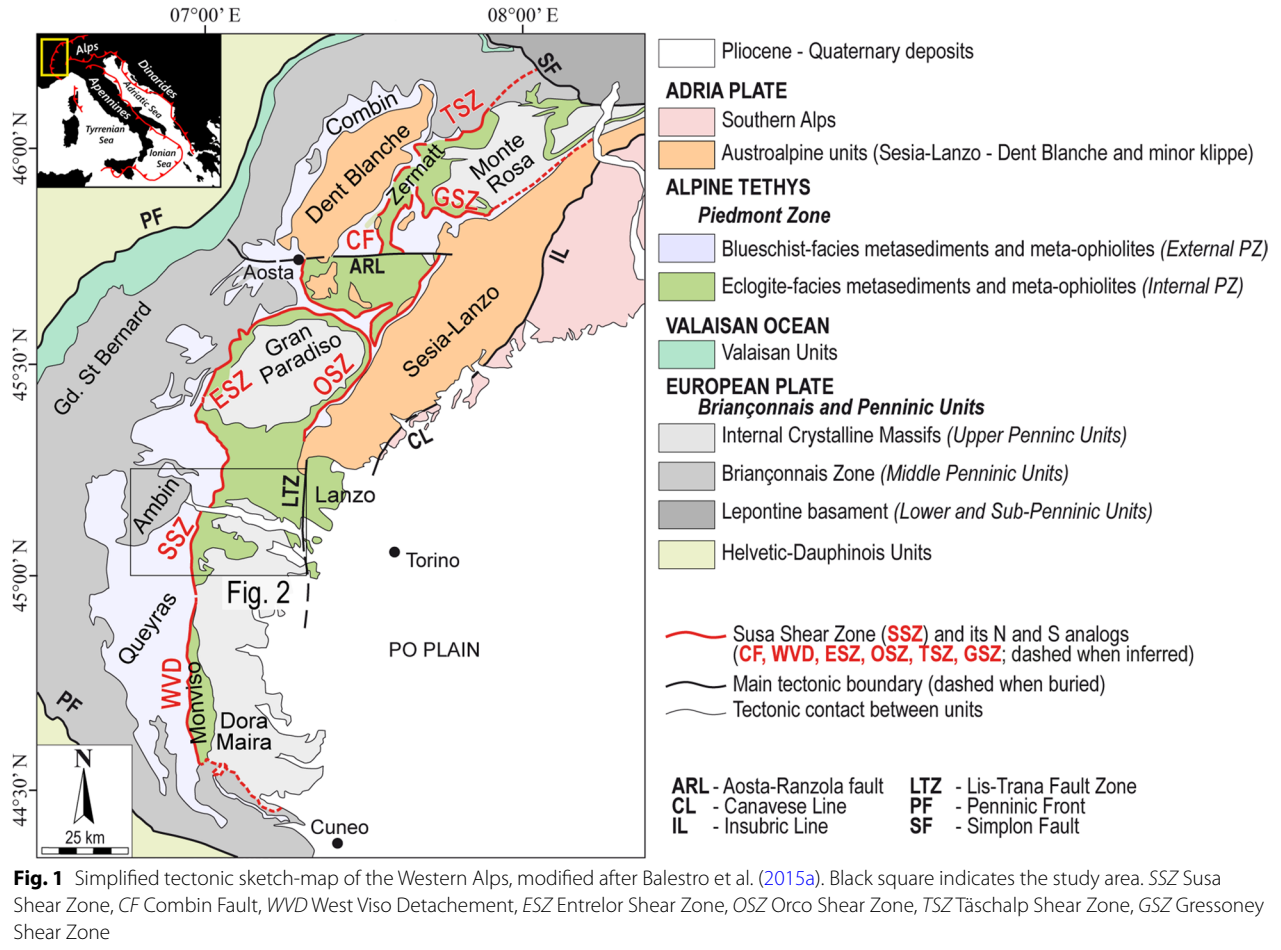

Fig. 1 Simplified tectonic sketch-map of the Western Alps, modified after Balestro et al. (2015a). Black square indicates the study area. *SSZ* Susa Shear Zone, *CF* Combin Fault, *WVD* West Viso Detachement, *ESZ* Entrelor Shear Zone, *OSZ* Orco Shear Zone, *TSZ* Täschalp Shear Zone, *GSZ* Gressoney Shear Zone

successions (i.e., the Gran San Bernardo System and the Briançonnais Zone; see e.g., Malusà et al. 2005; Strzerzynski et al. 2012 and references therein).

Tectonic contacts separating the IPZ and the overlying EPZ units, have been recognized all along the Western Alpine belt as polyphasic first-order shear zones. These shear zones are characterized by (i) a metamorphic gap between footwall (eclogite facies) and hangingwall (blueschist and greenschist facies), (ii) the occurrence of opposite kinematic indicators along similarly dipping shear planes, (iii) development under greenschist-facies metamorphic conditions and (iv) Eocene age of shearing (Ring 1995; Freeman et al. 1997; Reddy et al. 1999; Schmid and Kissling 2000; Cartwright and Barnicoat 2002; Ganne et al. 2006; Rosenbaum et al. 2012).

3 Geological setting of the Susa Valley

The different tectonic units exposed in the study area (Fig. 2a), from lower to higher structural levels, correspond to (i) the northern sector of the DM continental margin unit, (ii) the IPZ meta-ophiolite units, and (iii) the EPZ meta-ophiolite units. In the Susa Valley, the DM and the overlying IPZ were folded together during an early exhumation-related deformation phase and are separated from the EPZ by the SSZ, as shown in Fig. 2b. A panoramic view of the left slope of the Susa Valley is shown in Fig. 3, wherein different tectonic units and their geometrical relationships are highlighted.

3.1 Dora Maira unit

In the Susa Valley, the uppermost subunit of the DM occurs as defined by Vialon (1966), and Borghi et al. (1984), metamorphosed under eclogite-facies P–T peak conditions (i.e., P = 19 kbar and T = 510 °C; Gasco et al. 2011) and subsequently re-equilibrated under greenschist-to amphibolite-facies conditions, and its structural evolution was characterized by four main deformation phases (Gasco et al. 2011). The DM consists of a polymetamorphic basement (not exposed along the SSZ) and a metasedimentary Permo-Mesozoic cover (Sandrone et al. 1993; Cadoppi et al. 2002). The latter consists of a siliciclastic succession, which shows an upward transition

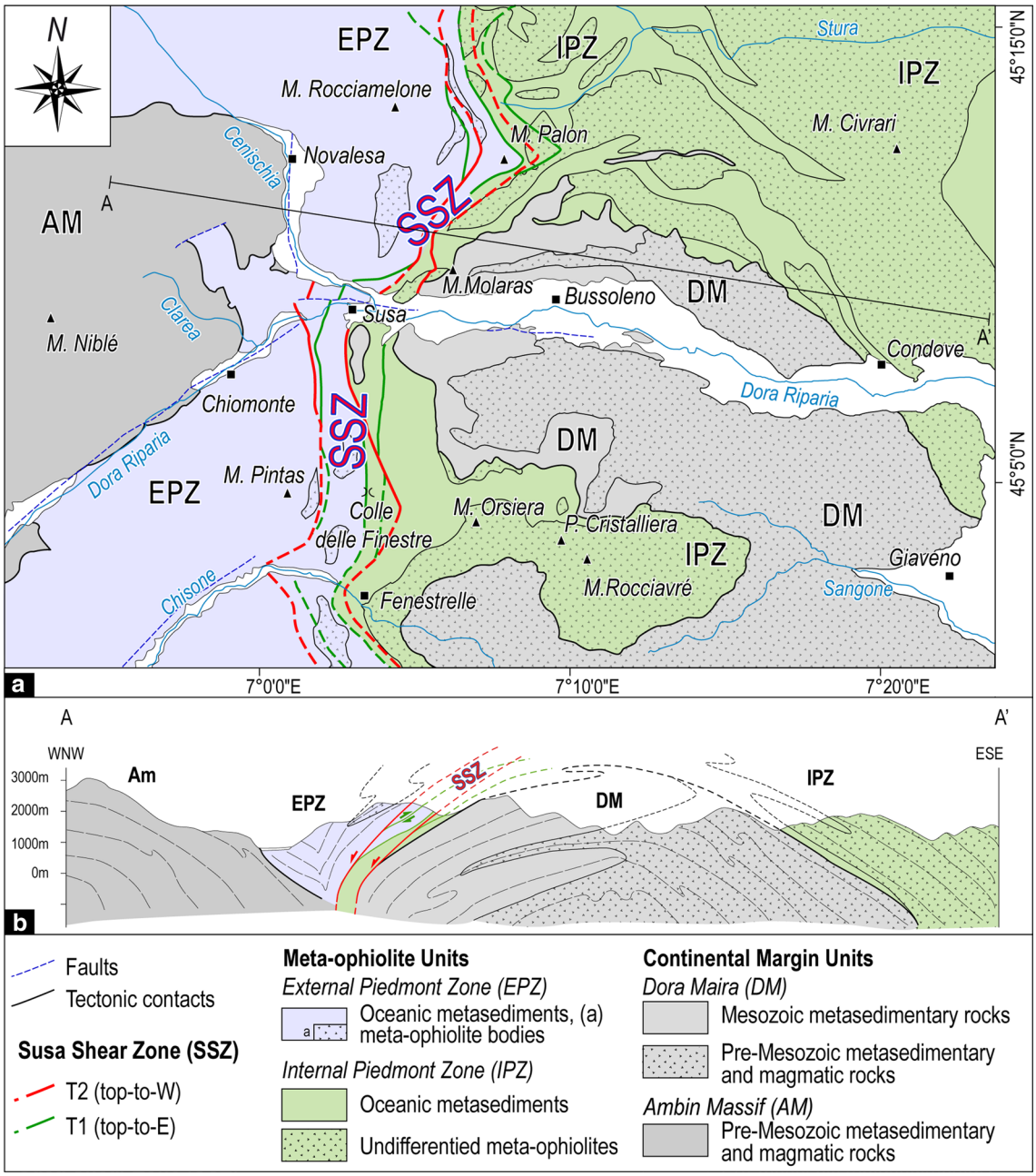

Fig. 2 **a** Simplified geological map of the axial sector of the Western Alps along the Susa Valley, **b** cross-section through the Susa Valley, showing the geometrical relationships between different tectonic units

to a carbonate one. Only the upper part of the metasedimentary Permo-Mesozoic cover (i.e., blocks of dolomitic marble) has been involved in the SSZ-related deformation (see Ghignone et al. 2020a).

3.2 Internal Piedmont Zone

The IPZ tectonically overlies the DM and, in the study area, consists of meta-ophiolites and related metasedimentary cover (i.e., the Orsiera-Rocciavrè Complex of Pognante 1979, and the Bassa Val di Susa-Valli di Lanzo-Monte Orsiera Unit of Cadoppi et al. 2002) and was metamorphosed under eclogite-facies P–T peak conditions (i.e., P = 25–29 kbar and T = 460–510 °C, Ghignone et al. 2020b) and during exhumation were re-equilibrated under greenschist-to-amphibolite facies conditions. The IPZ consists of serpentinized

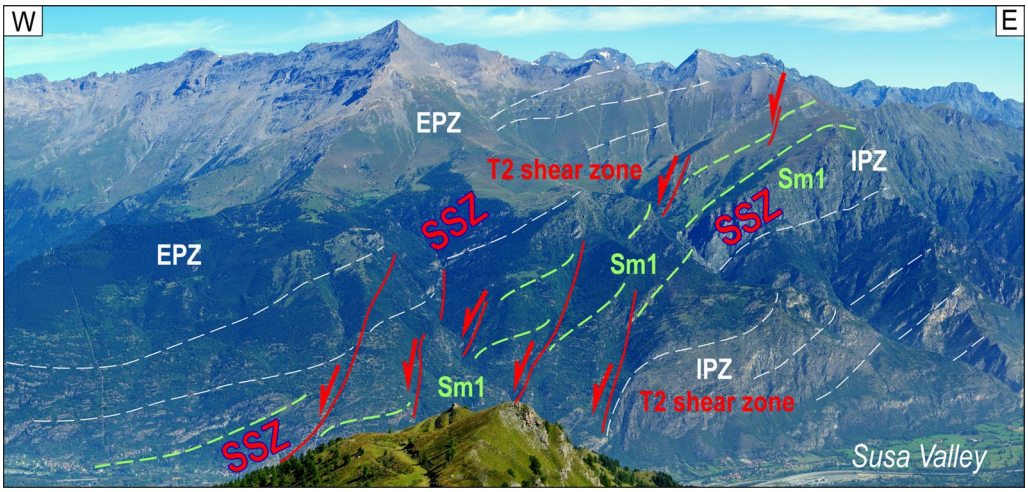

Fig. 3 Panoramic view of the left slope of the Susa Valley (SSZ highlighted), showing the geometric relationships between T1 and T2 shearing events. Dashed green lines: T1-related mylonitic foliation (Sm1); red lines with arrows: T2-related discrete shear bands; dashed white lines: S2 regional foliation

metaperidotite, metagabbro, metabasalt and metasediments (Nicolas 1966). Metaperidotite is of lherzolitic origin and was intruded by bodies of Mg–Al metagabbro and Fe–Ti metagabbro (Leardi and Rossetti 1985), whereas metabasalt locally shows relics of breccia- and pillow-lava structures. The metasedimentary cover mainly consists of calcschist of supposed Late Cretaceous age (Marthaler et al. 1986). Serpentinite usually shows a massive structure but appears as strongly foliated serpentine schist along tectonic contacts and particularly along the SSZ, whereas metagabbro and metabasalt are generally less deformed.

3.3 External Piedmont Zone (EPZ)

In the Susa Valley, the EPZ consists of different tectonic units (e.g., the Puys-Venaus Unit of Polino et al. 2002), made up of metasediments of oceanic origin (i.e., the Schistes Lustrés; Deville et al. 1992, and references therein) which embed bodies of meta-ophiolite. The EPZ records a metamorphic evolution defined by a P–T peak under blueschist-facies conditions and a subsequent re-equilibration under greenschist-facies conditions (P = 12–13 kbar and T = 350 °C, Agard et al. 2001 and references therein).

The meta-ophiolite consists of serpentinized metaperidotite, serpentine schist, metagabbro and metabasalt. The metasedimentary cover is mainly made up of a thick calcschist succession. The latter is interbedded by paragneiss, micaschist and quartzite (i.e., the Charbonnel Gneiss of Michel 1953; Pognante 1983), ranging from meter- to hundred-of-meter thick lenticular bodies. In the study area, the EPZ tectonically overlies both the IPZ and the Ambin Massif (see Lorenzoni 1968; Borghi and Gattiglio 1997; Borghi et al. 1999 and references therein), a Briançonnais-like continental margin unit.

4 Structural evolution

The tectonic units outcropping in the study area were deformed during subduction- and exhumation-related Alpine history, recording four main regional deformation phases, from D1 to D4. The polyphasic Susa Shear Zone (SSZ), was characterized by two distinct shearing events (T1 and T2 hereafter). Some outcrop-scale structures related to the main deformation stages are reported in Fig. 4 (details below), while the orientation of the different structural elements characterizing the deformation stages are shown in Fig. 5 (see details below). As shown in Fig. 6f, the shearing events in the SSZ (T1 and T2) were nearly coeval with regional folding and weaker shearing in the neighbouring rocks (D2 and D4).

4.1 Regional deformation phases

It should be emphasized that the pre-coupling structural evolution may have been different between the tectonic units (DM, IPZ and EPZ), while the post-coupling deformation history was common. Therefore the older tectonic phases (D1 and early D2), although presenting similar deformation and kinematic features, likely developed at different crustal levels, metamorphic and tectonic conditions.

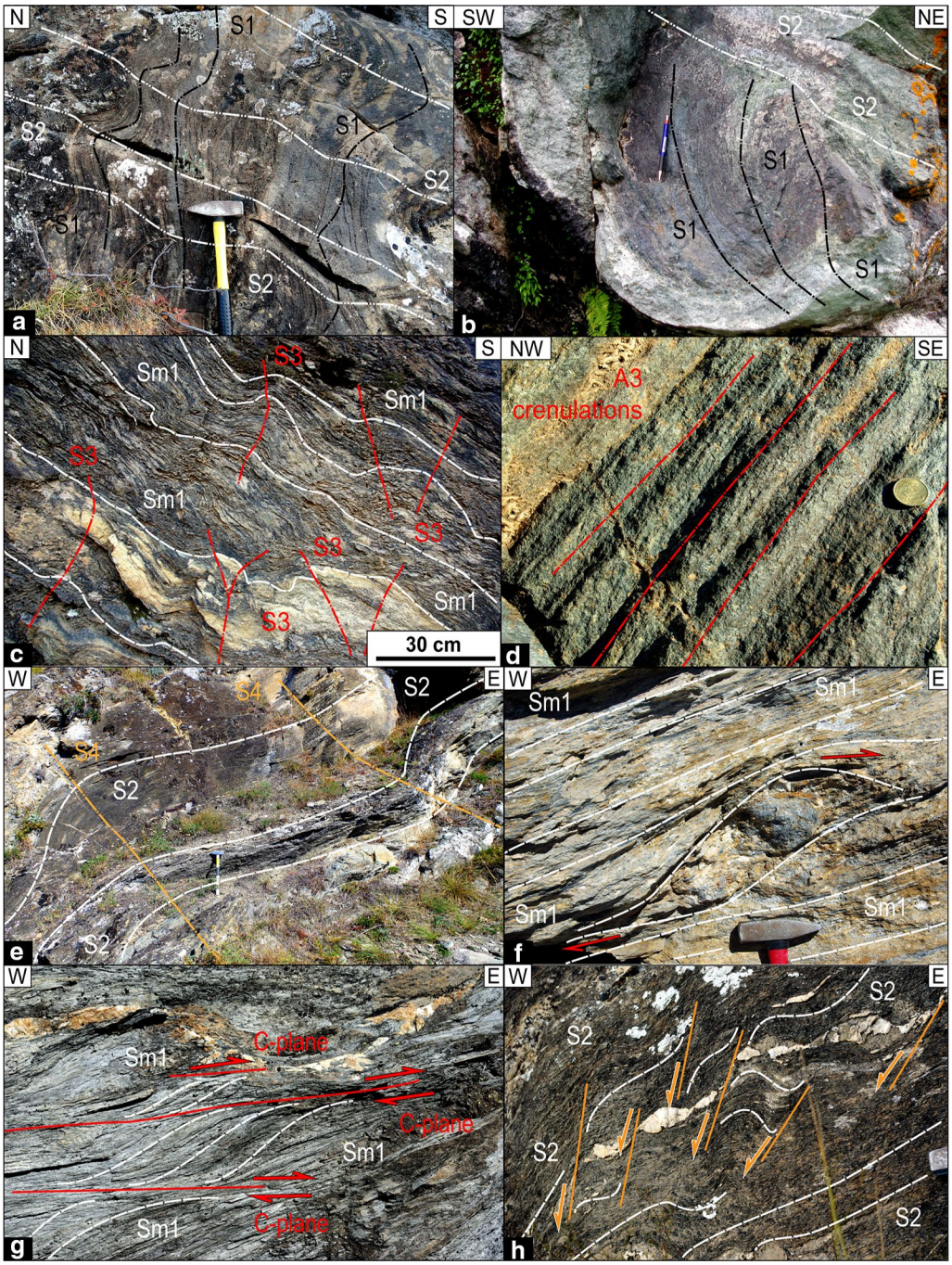

Fig. 4 Images of different field-scale structures. Interference relationships between S1 (dashed black lines) and S2 (dashed white lines) folds in **a** calcschist + paragneiss in EPZ and in **b** metagabbro + serpentinite in IPZ. **c** D3 box-folds (conjugated S3 axial planes dashed red lines) deforming Sm1 mylonitic foliation (dashed white lines) in the mylonitic calcschist of the SSZ. **d** A3 (dashed red lines) crenulation lineations in metabasalt. **e** D4 folds (S4 axial planes dashed orange lines) deforming S2 regional foliation (dashed white lines) in calcschist of the IPZ. **f** T1-realted Top-to-E shear sense marked by a sigma-shaped exotic block wrapped by the Sm1 mylonitic foliation (dashed white lines) in the mylonitic calcschist of the SSZ. **g** T1-related kinematic indicators (Top-to-E C-planes in red, Sm1 dashed white lines) in mylonitic calcschist. **h** T2-related S–C structures (C-planes in orange) showing Top-to-W kinematism deforming S2 regional foliation (dashed white lines), in calcschist of the IPZ

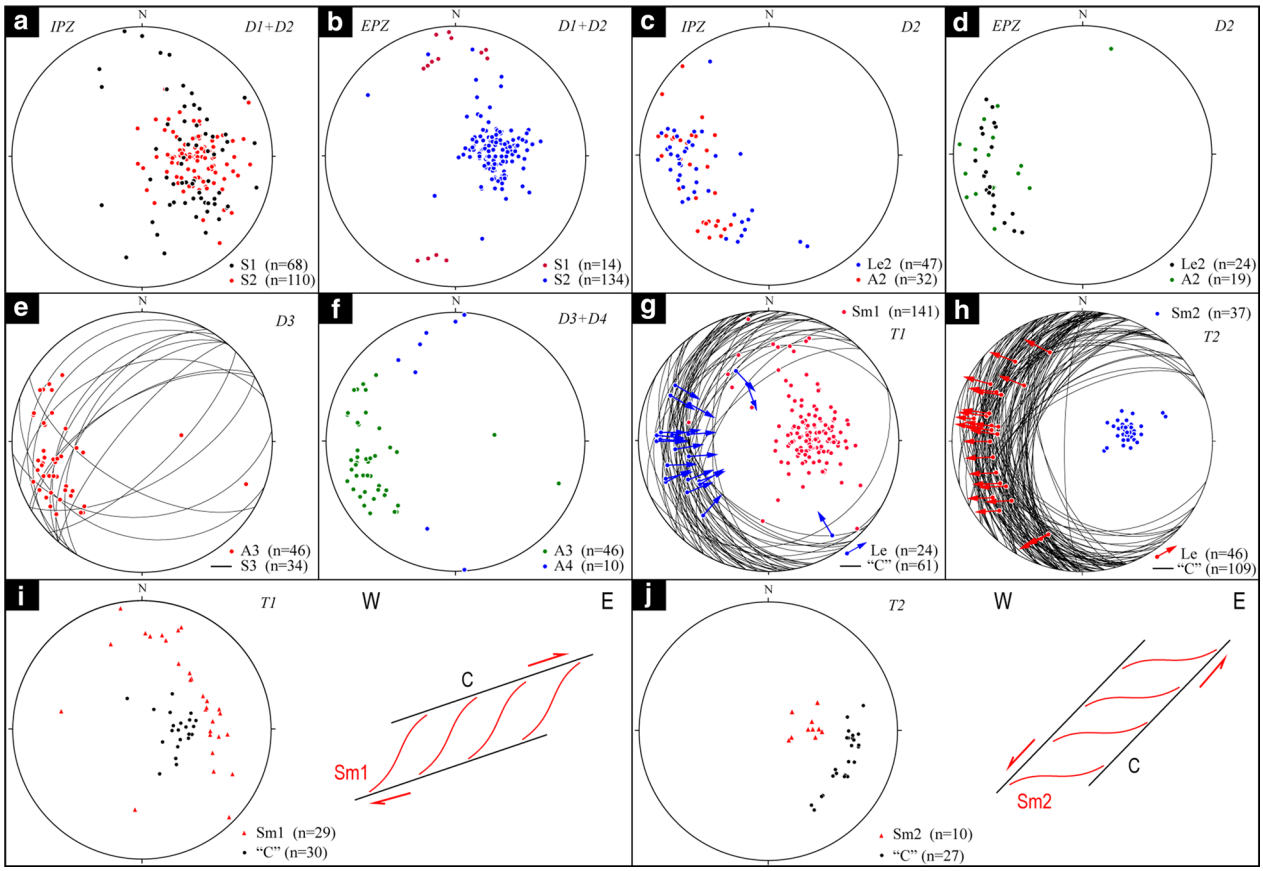

Fig. 5 Equal-area lower-hemisphere projections of different structures (n: number of data): **a** poles of S1 and S2 foliations from the IPZ, and **b** from the EPZ. **c** D2-related lineations from the IPZ: stretching lineations (Le2) in blue, fold axis (A2) in red, and **d** D2-related lineations from the EPZ: stretching lineations (Le2) in black, fold axis (A2) in green. **e** D3-related structural elements from both IPZ and EPZ: great circles represent S3 axial plane foliation, red dots represent A3 fold axes. **f** D3 and D4 fold axes (A3 in green and A4 in blue). **g** Great circles of T1-related shear planes ("C") and poles of the Sm1 mylonitic foliation (all data), and **h** great circles of T2-related shear planes ("C") and poles of the Sm2 disjunctive cleavage (all data) from the SSZ (blue and red arrows indicate T1- and T2-shear senses, respectively, stretching lineations on "C" planes). **i** Poles of T1-related shear planes ("C", black dots) and Sm1 mylonitic foliation (red triangles) of significant relationships on the field (data already contained in **g**), and **j** poles of T2-related shear planes ("C", black dots) and Sm2 disjunctive cleavage (red triangles) from the SSZ of significant relationships on the ground (data already contained in **h**)

4.1.1 D1

D1 phase is only discontinuously preserved, and testified by mesoscopic relics of different structural elements. This deformation phase developed under HP conditions, in particular the DM and IPZ record D1 during eclogite-facies conditions as reported by Ghignone et al. (2020b), while the EPZ was affected by D1 deformation phase under blueschist-facies conditions (Agard et al. 2001).

S1 metamorphic foliation is the most pervasive foliation in each tectonic unit, but its fabric, almost completely overprinted by S2 regional foliation, is preserved only locally (e.g., marble of the DM, metagabbro of the IPZ and paragneiss of the EPZ), or it is identifiable as deformed surface in D2 fold hinges (Fig. 4a, b). Locally, especially in the IPZ, S1 is developed as a metamorphic layering. D1 folds are rootless structures showing elongated isoclinal limbs, sharp hinges and asymmetric geometry (in both the IPZ and EPZ). In the whole study area, A1 fold axes are mainly defined by intersection lineations, while Le1 stretching lineations are defined by elongated metamorphic minerals (e.g., phyllosilicates in marbles, chloritoid in metapelites). A1 and Le1, are about N-S trending and parallel to each other in both the IPZ and EPZ. This is in line with the presence of D1 sheath folds exposed with typical *anvil-* or *eye-shaped* sections on rock surfaces (Mies 1993), in both the IPZ and EPZ. In the IPZ, S1 is almost N–S striking and W dipping (Fig. 5a); in the EPZ, S1 is E–W striking, dipping both to N and to S (Fig. 5b). This different S1 orientation in the two tectonic units could be due to its different

development between the tectonic units, or to different development of the subsequent D2 deformation, which re-oriented D1 structural elements.

At the bottom of the IPZ, relics of the tectonic contact responsible for the early coupling with the DM (not detailed in this work; see Gasco et al. 2011 for further details) are present. This tectonic contact is marked by an almost fully recrystallized shear zone, along which several tectonic blocks, belonging to both adjacent tectonic units, are preserved. This tectonic contact was folded by D2 folds and developed between D1 and D2 (Gasco et al. 2011).

4.1.2 D2

The main structures developed in the study area are due to D2 deformation phase. The latter developed under greenschist-facies re-equilibration in the IPZ, as also reported by Gasco et al. (2011) for the DM Massif, coupled with the IPZ. Also in the EPZ, D2 developed under greenschist-facies conditions (Agard et al. 2001).

D2 folds show isoclinal profile in the IPZ, whereas close to tight geometry is common in the EPZ. D2 folds developed inside the units, as shown in Fig. 6a, b, away from the boundary of the units. In both tectonic units, D2 re-fold previous structural elements, developing a pervasive S2 axial plane foliation, which represents the regional foliation in the study area. In detail, S2 developed well in lithologies where phyllosilicate content is abundant, whereas in other lithologies, such as metagabbro and marble, S2 is represented by discrete surfaces, developed in the D2 fold hinges. S2 dips to W (mainly to NW-SW in the IPZ and to W-WNW in the EPZ) at low to moderate angle (Fig. 5a, b). In the IPZ S1 and S2 are quite parallel each other, due to parallelizing of fold limbs to D2 axial planes (Fig. 5a). Accordingly, S1 + S2 is considered as a composite foliation. Contrary, in the EPZ, the average orientation values of the two foliations are almost perpendicular, depending on the more open geometry of D2 folds (Fig. 5b). A2 fold axes are mainly represented by intersection and minor crenulation lineations, while Le2 stretching lineations are underlined by elongated minerals on S2 fabric (e.g., green amphibole in metabasalt). In the IPZ and EPZ, A2 and Le2 are both oriented E-W, and almost parallel each other, as observed in well-preserved *anvil-shaped* folds within marble and paragneiss at the meso-scale and of *eye-shaped* folds (Mies 1993) within calcschist and dolomitic marble at the macro-scale (Fig. 5c, d). These features testify the occurrence of non-cylindrical folding during D2, probably developed in non-coaxial deformation (Brun and Merle 1988). These structures are evident from the outcrop scale to map scale. The non-cylindrical shape of these folds is particularly evident around M. Molaras (see Ghignone et al. 2020a), where they appear as double-verging folds along their axial plane, assuming the characteristic of *eye-shaped* folds.

In both the IPZ and EPZ, kinematics indicators (e.g., porphyroclasts along S2 foliation, such as pre-kinematic garnet, omphacite, chloritoid, and quartz aggregates) observed in outcrop corresponding to XZ plane of D2 strain, show Top-to-W shear sense, indicating a general westward tectonic transport (vergency) during D2 deformation. D2-related vergency observed inside the tectonic units, along the S2 axial plane foliation, was inferred considering the geometry of the subsequent deformation phases (D3 and D4), which re-oriented D2 structures, as observed in the western sector of the IPZ, where S2 foliation dips to the West and original D2 synclines presently appear as antiforms (see cross-section in Fig. 2b).

The relationships between D2 and SSZ (T1) and their relative timing are discussed below.

4.1.3 D3

The orientation of the D3 structural elements and their tectonic meanings are common in the DM, IPZ and EPZ, as well as for the interposed mylonitic rocks (SSZ) responsible for their coupling. The geometry of D3 folds depends on the different rheological behavior of deformed rocks, varying from open folds in marble, gneiss and metabasalt, to close folds in calcschist, micaschist and serpentine schist. These features include common cusps and lobes morphology. D3 folds are generally characterized by asymmetric geometry, with long and short limbs, locally overturned, and D3 folds occur at all scales, re-orienting previous structures. Box-folds related to D3 also occur, with conjugated axial planes mostly dipping to N and less often to S (Fig. 4c). Along mesoscopic hinges, A3 axes are well developed as pervasive crenulation lineations (Fig. 4d), mainly WSW-ENE trending and west-plunging at low to medium angle. Due to the partly different orientation of the box-folds, minor A3 axes oriented WNW-ESE are present (Fig. 5e).

(See figure on next page.)

Fig. 6. 2D-schematic sketches showing the geometry and relationships between deformation phases: **a** pre-coupling D1 and D2 folds geometry inside EPZ unit; **b** D2-related deformation of the IPZ/DM tectonic contact (blue line) and D2 folds geometry inside coupled IPZ and DM unit; **c** T1 coupling between IPZ + DM and EPZ, and related Top-to-E shear zones (green lines; see text); **d** D3 folds re-orienting previous T1 shear zone; **e** D4 folds and coeval T2 shear zones superposed T1 shear zones; **f** Summary of deformation relative timing, highlighting the nearly coeval development of the shearing events with D2 and D4 folding phases

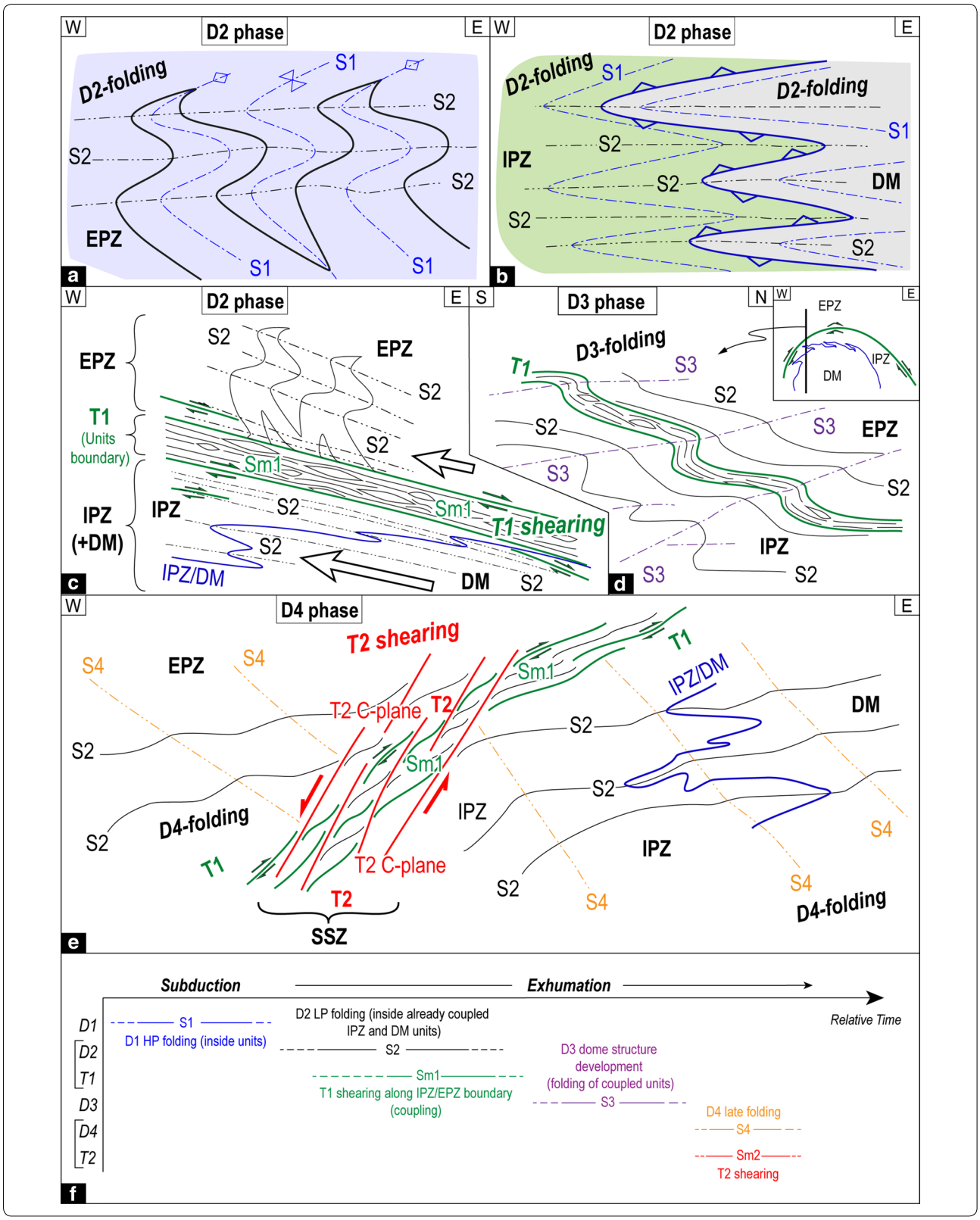
W
D2 phase
E
D2-folding
S1
S2
EPZ
a
IPZ
DM
b
D3 phase
S
N
D3-folding
T1
S3
T1 shearing
Sm1
IPZ/DM
c
d
D4 phase
T2 shearing
S4
T2-C-plane
T2
T2 C-plane
D4-folding
SSZ
e
Subduction
Exhumation
Relative Time
D1
D2
T1
D3
D4
T2
D1 HP folding (inside units)
D2 LP folding (inside already coupled IPZ and DM units)
T1 shearing along IPZ/EPZ boundary (coupling)
D3 dome structure development (folding of coupled units)
D4 late folding
Sm2
T2 shearing
f

Vergency of D3 folds is mainly northwards, even if, locally, parasitic folds of inverted D3 fold limbs have southward vergence. S3 axial plane foliation is not pervasive and mainly developed in calcschist and micaschist as a disjunctive crenulation cleavage, mostly dipping to NW. In addition, syn-D3 shear zones locally occur, defined by meter-thick mylonitic to cataclastic rocks. These shear zones accommodate the D3 deformation, showing Top-to-N shear sense, coherent with D3 vergency.

4.1.4 D4

D4 is the latest ductile regional phase, developed at shallow structural levels, as testified by the geometry of folds, which are variably open, without developing pervasive axial plane foliations or cleavages. These folds, never overturned, show asymmetric geometry (Fig. 4e) with NNW-SSE trending axes (A4), gently plunging northwards (5–10°, Fig. 5f). Their axial plane, always very steep, is directed approximately N–S and defined by spaced disjunctive cleavage (S4). These folds, recognizable from mesoscopic to map scale, show widespread Top-to-W vergency, causing a diffused westward lowering of all tectonic surfaces and lithological contacts. Locally, along D4 folds short limbs, discrete shear bands with Top-to-W shear sense occur.

4.2 Susa Shear Zone (SSZ)

As previously stated, the IPZ, EPZ and, in part, the DM were coupled through the SSZ, which developed during two distinct shearing events (T1 and T2). A mylonitic foliation (Sm1) developed during T1 event, whereas a disjunctive cleavage (Sm2) developed during T2 event. The inner tectonic architecture of the SSZ is arranged as a tectonic mélange (sensu Festa et al. 2019), mainly consisting of a calcschist matrix wrapping blocks sampled from the units in contact. The superposition of the two shearing events has progressively increased this block-in-matrix structure. The entire rock volume affected by the superposed T1 and T2 deformation varies in thickness from some hundreds of meters, in the northern slope of the Susa valley, to about one kilometer in the southern one. A pervasive mylonitic foliation developed in calcschist, micaschist and serpentine schist, whereas metabasalt, metagabbro and paragneiss blocks are wrapped by this mylonitic foliation, and partly disrupted in domino structures (sensu Goscombe and Passchier 2003). Upper and lower boundaries of the shear zone appear commonly not sharp. In particular, moving toward the EPZ, the mylonitic foliation and the superposed shear bands are less and less pervasive, more spaced and often concentrated in discrete m-sized deformation bands. Moving toward the IPZ, the deformation also decreases, as testified by the occurrence of thinner shear bands in which deformation is concentrated. The geometric relationships between T1 and T2 are reported in Fig. 6e.

4.2.1 T1

The first shearing event (T1) gave rise to a thick shear zone, on average NNE-SSW striking, showing a block-in-matrix structure. The strongly deformed matrix (i.e., mylonitic calcschist) embeds blocks sliced from the IPZ, EPZ and, to a lesser degree, from the DM (e.g., metabasalt, massive serpentinite, paragneiss, dolomitic marble and metagabbro, Fig. 4f). Sm1 is strongly pervasive and transpositive, millimetre-spaced in the calcschist. Sm1 overprints previous lithological textures, giving the rocks a homogeneous appearance. This homogenization is particularly evident in calcschist (Fig. 4g), wherein the original carbonate-rich and phyllosilicate-rich layering, occurring in the non-mylonitic calcschist of both the IPZ and EPZ, disappears. The dip of Sm1 is quite scattered towards NW to SW (Fig. 5g), resulting on average about sub-parallel to S2 regional foliation. Geometrical field relationships between Sm1 and S2 are not always univocal: Sm1 was usually observed to cut S2 at low angle (< 10°), and locally the two foliations are parallel to each other, distinguished on the basis of a local strain increase. These structural relationships suggest that Sm1 and S2 developed nearly coeval, in different domains. Sm1 developed as mylonitic foliation at the boundary between the lower IPZ + DM and the upper EPZ during syn-to-late-D2 deformation event, while S2 developed as axial plane foliation inside the tectonic units.

Kinematic indicators occurring within the Sm1 correspond to S–C (C′) fabric, δ- and σ-type mantled porphyroclasts and overturned folds. In particular, extensional crenulation cleavage (ECC) and C planes (sensu Platt and Vissers 1980) are the most abundant kinematic indicators (Fig. 4g), concentrated in sets of millimeters to meters-spaced discrete shear bands.

Kinematic indicators provide a Top-to-E "apparent reverse" sense of shear (Fig. 5i). C planes dip from NW to SW (Fig. 5g) showing dispersion similar to the mylonitic foliation. Stretching lineations underlined by elongated minerals and occurring on the C planes roughly plunge parallel to the dip of C planes (Fig. 5g). The long axis of the blocks (of every size) is parallel to the stretching lineations measured on the C planes.

All the structural elements related to T1 show the same dispersion, because of their re-orientation during the D3 regional folding phase (see Fig. 5e, g for comparison between D3 and T1 structural elements, and Fig. 4c field relationships).

4.2.2 T2

The second shearing event (T2) developed a hundred-meter-thick deformation zone, on average N–S striking and W-dipping, which crosscuts previous structures, giving rise to a reworked tectonic mélange. Sm2 is a disjunctive cleavage, different from the previous Sm1, concentrated along discrete and spaced shear bands. These are defined by bands of ECC and occur more pervasive and less spaced closer to the IPZ, while, moving towards EPZ, these discrete shear bands becomes progressively more spaced and wrapping tectonic blocks of various size. Usually, T2-related blocks are bigger than the T1-related ones and more disrupted. Sm2-C kinematic indicators (Fig. 5h) dip both toward W, almost parallel, varying their angle of dip. T2-related shear bands show fairly constant dip values and orientations, while C-planes vary from subhorizontal to medium-angle dipping to SW and NW. This wide range of values can be related to different orientations of the C-planes around tectonic blocks, also explaining the wide dispersion of stretching lineation on these planes. T2 kinematic indicators (e.g., ECC, S–C structures and rotated porphyroclasts) are consistent with Top-to-W sense of shear (Fig. 5l). S–C planes of the two shearing events show relations of superposition and cross-cutting, T2-related C planes crosscut and reorient T1-related C planes). Sm2 wraps lithons containing T1 kinematic indicators, and locally, T2-related C planes overprint and completely erase previous structural elements (Fig. 6e). On outcrop and map scale, the relative movement of footwall and hanging wall causes the downward bending of previous contacts in the footwall (Fig. 4h). T2-related structural elements are not involved in the regional folding phases, suggesting their development coeval with D4 regional deformation phase. This is consistent with T2-related shear bands developed along short limbs of D4-related folds, as stated before.

T2-related kinematic indicators occur more pervasively along the N slope of the Susa Valley, with cm- to m-spaced ECC shear bands, while in the southern one the shear bands are more spaced (tens of m). This is likely due to the interference with the adjacent Ambin Massif, present only in the northern slope and absent in the southern one.

5 Discussion

5.1 Tectonic evolution of the SSZ

The tectonic history recorded along the SSZ consists of two superposed steps (i.e., T1 and T2), whose relative timing is given by the relationships with the regional structures (D1 to D4, see Fig. 6f). The S1 + S2 composite foliation of the IPZ (Fig. 6b), and the S2 foliation of the EPZ (Fig. 6a) are the main structural markers. T1 drove the coupling between the IPZ, already coupled with the DM (Gasco et al. 2011), and the EPZ (Fig. 6c). The geometrical relationships between S2 and Sm1, highlight that D2 and T1 were nearly coeval, developing different structures and related kinematics within the tectonic units or along their boundary. Inside the IPZ and EPZ, S2 developed as axial plane foliation, with Top-to-W shear sense, while, along their boundary (i.e., the SSZ) the strain increased, developing the nearly coeval Sm1 mylonitic foliation, with Top-to-E shear sense.

After T1, the coupled tectonic elements suffered a regional folding (D3), tectonically linked with early development of a dome-like structure in the DM (see Gasco et al. 2013; Ghignone et al. 2020a). The original geometry of the T1 shear zones was then significantly re-oriented, as highlighted by the consistency between scattering of the Sm1 and orientation of D3 fold axes (Fig. 5e, g). D3 folds deformed, at the meso-scale, the T1 mylonites, tilting the original eastward plunging of the mylonites and the related kinematic indicators at the large scale, and giving the "apparent reverse" sense of shear. These structural relationships highlight that T1 tectonic developed before the D3 (Figs. 4c, 6d). Doming phases usually are related to folds with axes oriented concentric to the center of the dome and parallel to the border of the dome itself, with a centrifugal vergency (see e.g., Burg et al. 2004; Wang et al. 2015 and references therein). In the study area, D3 fold axes orientation (and related vergency) are consistent with these assumptions, due to their location along the NW flank of the DM dome-like structure. It is to emphasize that "apparent reverse" shear sense is probably related to this dome-related tilting which reoriented the original plunging of the T1-related shear zone, maintaining the same shear sense (Top-to-E normal fault).

During exhumation of tectonic units at shallower crustal levels, T2 structures developed and crosscut T1 shear planes. T2 structures accommodated a later phase of dome-related uplift of the DM and IPZ in the footwall of the SSZ, and the relative downthrow of the EPZ in the hanging wall, with a westward kinematics. The relative timing of the T2 is inferred to be syn-D4. At the mesoscale, T2 shear zones developed along short limbs of D4 folds, and, at the macroscale, they are in turn associated with D4 drag folds (Fig. 6e).

It is noteworthy that the tectonic elision of the IPZ south of the study area (see Fig. 1) likely corresponds to a maximum of exhumation of the underlying DM.

The tectonic evolution of the SSZ through time has been represented in a step-model (Fig. 7). The different steps reconstruct the tectonic evolution of the axial sector of the Western Alps along the Susa Valley, highlighting the geometrical relationships between the different tectonic units. In Fig. 7a the geological setting at late-D1

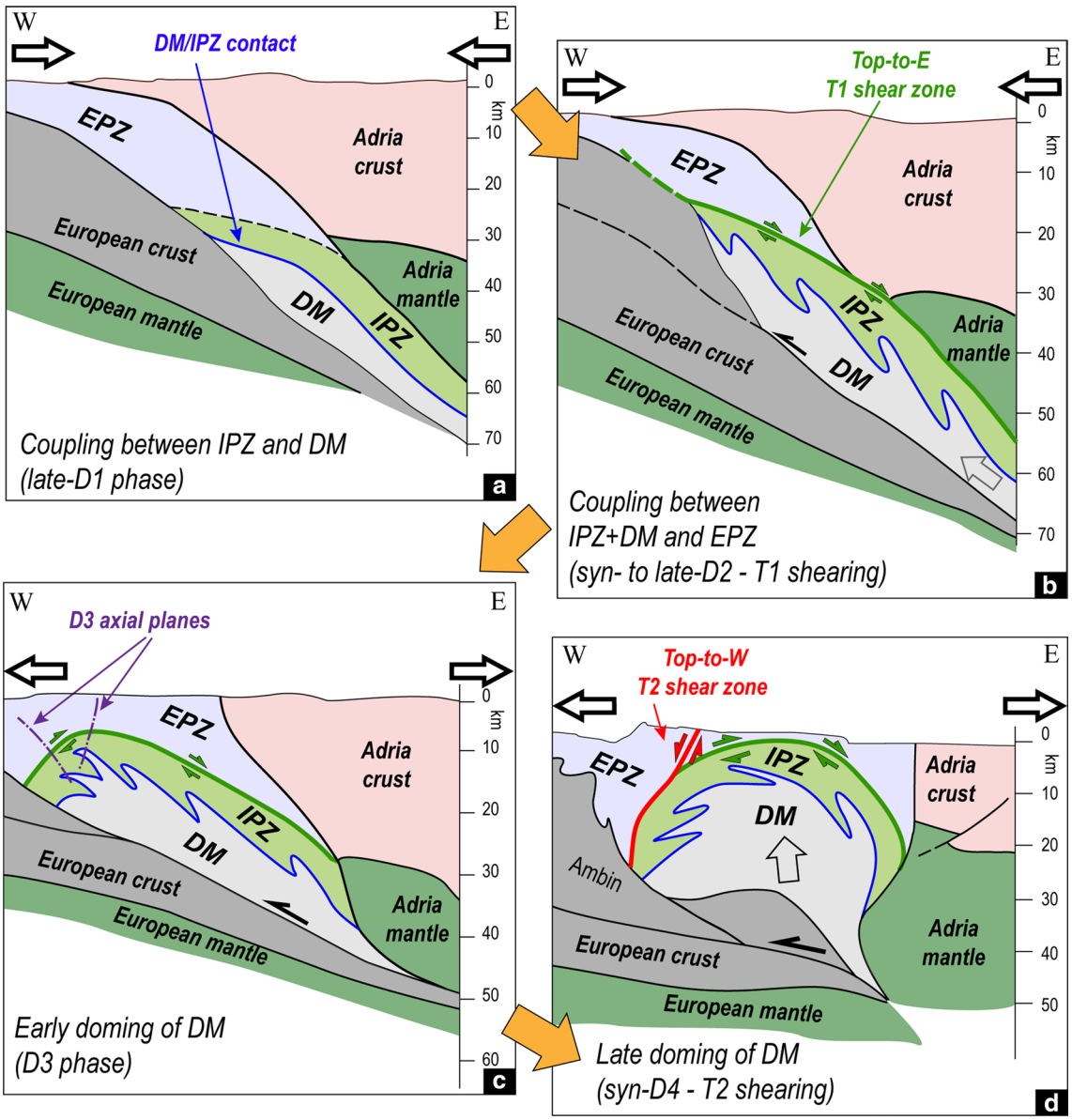

Fig. 7 Tectonic model of the evolution of the axial sector of the Western Alps along the Susa Valley (see text for details)

stage is represented, prior to the development of the SSZ. The IPZ was coupled through a thrust above the DM still in HP conditions. The IPZ and EPZ were probably not already adjacent each other (see dashed line along their contact, Fig. 7a), but this point still remains unclear. After the IPZ and DM coupling, the eclogite-bearing units were coupled with the upper blueschist-bearing units (EPZ), through the east-plunging T1-related shear zone, displaying Top-to-E kinematics (Fig. 7b). Different exhumation rates of the eclogite-bearing units with respect to the blueschist-bearing ones are inferred from the kinematics of the nearly coeval deformation events (syn- to late-D2), as represented in Fig. 6c (arrows indicate the different relative exhumation velocity). The subsequent D3 folding was related to the development of the dome-like structure of the eclogite-bearing units (Fig. 7c), which reoriented the previous structures, rotating the orientations of the surfaces from east-dipping to west-dipping in the study sector. The T2-related shear zone (Fig. 7d, red line) allowed the final uplift.

5.2 Comparison with other first-order shear zones

The polyphasic tectonics and the kinematics of the SSZ are discussed in the following by comparison with other shear zones that coupled tectonometamorphic units with different P–T metamorphic paths in the axial sector of the Alpine belt.

The occurrence of two distinct generations of kinematic indicators and of an important metamorphic jump from eclogite-facies footwalls to the greenschist- and blueschist-facies hanging walls has been widely reported along the Alpine belt (the Combin Fault by Ballèvre and Merle 1993; Ring 1995; Froitzheim et al. 2006; Pleuger et al. 2007; Kirst and Leiss 2017; the Susa Shear Zone by Gasco et al. 2013; Ghignone and Gattiglio 2013; Ghignone et al. 2020a; the Orco Shear Zone by Gasco et al. 2009; Gasco et al. 2013; the Gressoney shear zone by Reddy et al. 1999, 2003; Wheeler et al. 2001; Gasco et al. 2013; Savignano et al. 2016; the Täschalp shear zone by Barnicoat et al. 1995; Cartwright and Barnicoat 2002; the Entrelor shear zone by Butler and Freeman 1996; Rolland et al. 2000, Bucher et al. 2003; Malusà et al. 2005; Ganne et al. 2006; Rosenbaum et al. 2012; the West Viso Detachment by Ballèvre et al. 1990; Philippot 1990; Tricart et al. 2004).

All these cited shear zones are potential segments of one single coherent first-order regional-scale structure, because they are in the same tectonostratigraphic and tectonometamorphic position, as reported in Fig. 1.

Geochronological data constrain the timing of deformation along the Combin, Täschalp, Gressoney and Entrelor Shear Zones as Eocene, around 33–45 Ma (Barnicoat et al. 1995; Ring 1995; Freeman et al. 1997; Reddy et al. 1999; Schmid and Kissling 2000; Cartwright and Barnicoat 2002; Malusà et al. 2005; Rosenbaum et al. 2012). These Eocene ages are suitable for the timing of the T1 in the SSZ, considering the nearly coeval age of the D2 deformation in the Western Alps (Reddy et al. 1999; Dal Piaz et al. 2001).

T2 deformation of the SSZ, coeval with D4 deformation phase, likely developed in the Oligocene, according to the ages proposed by Balestro et al. (2009), and Perrone et al. (2010) for the D4 deformation phase.

The polyphase activity of previously mentioned shear zones was described by several authors, who reported early Top-to-E (SE) kinematics superposed by widespread later Top-to-W kinematics along the same contacts (Malusà et al. 2005; Ganne et al. 2006; Savignano et al. 2016). Reddy et al. (2003) inferred that the Top-to-SE kinematics played a major role in the structural history, responsible for the exhumation of the eclogite-facies units in the footwall of the Gressoney Shear Zone. In the same work, it was also pointed out that shear zones with normal-fault kinematics may have been tilted into orientations with apparent thrust geometry by later folding and shearing phases (Wheeler and Butler 1993; Butler and Freeman 1996; Ring 1995; Ganne et al. 2006; Pleuger et al. 2007). The occurrence of the "apparent reverse" sense of shear (i.e., re-folded early shear zone) has been documented by Barnicoat et al. (1995), Bucher et al. (2003), Ganne et al. (2006), Gasco et al. (2009), Ghignone et al. (2020a), and related to the doming of the ICM.

Philippot (1990) also reported the presence of discrete shear bands, including both Top-to-E and Top-to-W kinematic indicators.

The former nature of early shear zones was interpreted either as folded normal faults or as folded thrusts. Rolland et al. (2000), Wheeler et al. (2001), and Tricart et al. (2004) interpreted the shear zones as characterized by a single event of normal faulting.

Philippot (1990), and Ballèvre et al. (1990) proposed the occurrence of backthrusting for the West Viso Detachment, wherein two opposite kinematic indicators were referred to a coeval deformation stage. Butler and Freeman (1996) also support the hypothesis of backthrusting along the Entrelor Shear Zone, which involves the Gran Paradiso Massif and the Piedmont Zone.

Furthermore, Froitzheim et al. (2006), and Pleuger et al. (2007) interpreted the Combin Fault as a normal fault that formed during downward extraction of a larger rock volume above the exhuming eclogite-bearing unit and subsequent out-of-sequence thrusting.

Ballèvre and Merle (1993) suggested that early Top-to-E kinematic developed along a normal fault (i.e., the Combin fault), which was reactivated during Top-to-W shearing.

6 Orogen scale implications and conclusions

As already inferred, SSZ is a first-order tectonic contact, mostly developed within the meta-ophiolitic units of the Piedmont Zone (i.e., the IPZ and EPZ), tectonically overlying the ICM (i.e., the DM in the study area) and the Gran San Bernardo nappe system (i.e., the Ambin Massif in the study area). During the T1 event, the already coupled DM and IPZ were exhumed below the EPZ in the form of an extruding wedge structure, bounded by a normal fault, such as the SSZ, at its top and a by thrust, at its base, likely deep-rooted and associated with the Frontal Pennidic Thrust.

We propose a general common evolution for the system of different shear zones, which drove exhumation of different tectonic units within the axial sector of the Western Alps. As a matter of fact, each of these shear zones was characterized by two shearing events. A first shearing event (Top-to-E, T1 of the SSZ) exhumed the already coupled ICM + IPZ units below the EPZ units, which were both moving away from the upper plate

towards the foreland during Late Eocene shortening. T1 shear zones were dipping towards the hinterland, displaying an exhumation-related "extensional" Top-to-the foreland kinematics. "Extensional kinematics" would thus result from different exhumation rates, which should be higher for the IPZ + DM, and lower for the EPZ. In this interpretation, T1 shear zones are clearly part of an exhumation-related normal fault (Butler et al. 2013), in a system similar to the "pip" model proposed by Wheeler et al. (2001).

When the second shearing event occurred (T2 of the SSZ), during a main phase of doming, resulting shear zones then developed with a centrifugal kinematics with respect to the center of the dome-like structures. Accordingly, it is possible to suggest a later vertical motion of the composite eclogite-bearing continental-oceanic crust (ICM and IPZ) beneath the blueschist–greenschist-bearing one (EPZ). In this view, a HP–LT metamorphic dome occurred in the axial position of the Western Alps orogenic wedge: the ICM (and the IPZ, when present) behave as core complexes, and the shear zones developed along their flanks were the weak zones that accommodated the doming itself.

Acknowledgements
We thank Editors Stefan Schmid, Daniel Marty and Paola Manzotti for the careful editorial handling, Michel Ballèvre and Jan Pleuger for their constructive and thorough reviews.

Authors' contributions
Field work: SG, GB and MG; conceptualization: SG, GB, MG and AB; data collection: SG, GB and MG; data analysis: SG; methodology: SG, GB and MG; writing original draft: SG; figures draft and editing: SG, GB, MG and AB; validation: GB, MG and AB; writing, review and editing: SG, GB, MG and AB. All authors read and approved the final manuscript.

Funding
The research at the Department of Earth Science has been funded by Compagnia San Paolo and University of Turin in the frame of the GeoDIVE Project (A.B., S.G.), research grants from University of Torino, Ricerca Locale 'ex 60%' 2017–2018–2019 (A.B., G.B., M.G. and S.G.), and from the Italian Ministry of University and Research, 'Finanziamento annuale individuale delle attività base di ricerca' 2017 (GB).

Availability of data and materials
Not applicable.

Ethics approval and consent to participate
Not applicable.

Consent for publication
Not applicable.

Competing interests
The authors declare that they have no competing interests.

Received: 25 March 2020 Accepted: 5 October 2020
Published online: 28 October 2020

References

Agard, P., Jolivet, L., & Goffe, B. (2001). Tectonometamorphic evolution of the Schistes Lustrés complex: Implications for the exhumation of HP and UHP rocks in the Western Alps. *Bulletin de la Société Géologique de France, 172*, 617–636.

Agard, P., Monie, P., Jolivet, L., & Goffe, B. (2002). Exhumation of the Schistes Lustrés complex: *In situ* laser probe 40Ar/39Ar constraints and implications for the Western Alps. *Journal of Metamorphic Geology, 20*(6), 599–618.

Angiboust, S., Agard, P., Jolivet, L., & Beyssac, O. (2009). The Zermatt-Saas ophiolite: The largest (60-km wide) and deepest (c. 70–80 km) continuous slice of oceanic lithosphere detached from a subduction zone? *Terra Nova, 21*, 171–180.

Angiboust, S., & Glodny, J. (2020). Exhumation of eclogitic ophiolitic nappes in the W. Alps: New age data and implications for crustal wedge dynamics. *Lithos, 356–357*, 105374.

Balestro, G., Cadoppi, P., Perrone, G., & Tallone, S. (2009). Tectonic evolution along the Col del Lis-Trana Deformation Zone (internal Western Alps). *Bollettino della Società Geologica Italiana, 128*(2), 331–339.

Balestro, G., Festa, A., Borghi, A., Castelli, D., Tartarotti, P., & Gattiglio, M. (2018). Role of Late Jurassic intra-oceanic structural inheritance in the Alpine tectonic evolution of the Monviso meta-ophiolite complex (Western Alps). *Geological Magazine, 155*(2), 233–249.

Balestro, G., Festa, A., & Dilek, Y. (2019). Structural architecture of the Western Alpine Ophiolites, and the Jurassic seafloor spreading tectonics of the Alpine Tethys. *Journal of the Geological Society, 176*, 913–930.

Balestro, G., Festa, A., Dilek, Y., & Tartarotti, P. (2015a). Pre-Alpine extensional tectonics of a peridotite localized oceanic core complex in the late Jurassic, high-pressure Monviso ophiolite (Western Alps). *Episodes, 38*(4), 266–282.

Balestro, G., Festa, A., & Tartarotti, P. (2015b). Tectonic significance of different block-in-matrix structures in exhumed convergent plate margins: Examples from oceanic and continental HP rocks in Inner Western Alps (northwest Italy). *International Geology Review, 57*(5–8), 581–605.

Balestro, G., Lombardo, B., Vaggelli, G., Borghi, A., Festa, A., & Gattiglio, M. (2014). Tectonostratigraphy of the northern Monviso meta-ophiolite complex (Western Alps). *Italian Journal of Geosciences, 133*(3), 409–426.

Ballèvre, M., Lagabrielle, Y., & Merle, O. (1990). Tertiary ductile normal faulting as a consequence of lithospheric stacking in the Western Alps. *Mémoire Societé Géologique de France, 156*, 227–236.

Ballèvre, M., & Merle, O. (1993). The Combin fault: Reactivation of a detachment fault. *Schweizerische Mineralogische und Petrologische Mitteilungen, 73*, 205–227.

Barnicoat, A. C., Rex, D. C., Guise, P. G., & Cliff, R. A. (1995). The timing of and nature of greenschist facies deformation and metamorphism in the upper Pennine Alps. *Tectonics, 14*(2), 279–293.

Bearth, P. (1967). Die Ophiolithe der Zone von Zermatt-Saas Fee. *Beiträge zur Geologischen Karte der Schweiz, Neue Folge, 132*, 130.

Beltrando, M., Compagnoni, R., & Lombardo, B. (2010). (Ultra-) high-pressure metamorphism and orogenesis: An Alpine perspective. *Gondwana Research, 18*(1), 147–166.

Borghi, A., Cadoppi, P., Porro, A., Sacchi, R., & Sandrone, R. (1984). Osservazioni geologiche nella Val Germanasca e nella media Val Chisone (Alpi Cozie). *Bollettino del Museo di Scienze Naturali, Torino, 2*, 503–530.

Borghi, A., & Gattiglio, M. (1997). Osservazioni geologico-petrografiche nel settore meridionale del Massiccio d'Ambin. *Atti Ticinesi di Scienze della Terra, 5*, 65–84.

Borghi, A., Gattiglio, M., Mondino, F., & Zaccone, G. (1999). Structural and metamorphic evidence of pre-alpine basement in the Ambin nappe (Cottian Alps, Italy). *Memorie di Scienze Geologiche, Padova, 51*(1), 205–220.

Brun, J. P., & Merle, O. (1988). Experiments on folding in spreading-gliding nappes. *Tectonophysics, 145*(1–2), 129–139.

Bucher, K., Fazis, Y., De Capitani, C., & Grapes, R. (2005). Blueschists, eclogites, and decompression assemblages of the Zermatt-Saas ophiolite: High-pressure metamorphism of subducted Tethys lithosphere. *American Mineralogist, 90*, 821–835.

Bucher, S., Schmid, S. M., Bousquet, R., & Fugenshuh, B. (2003). Late stage deformation in a collisional orogen (Western Alps): Nappe refolding, back thrusting or normal faulting? *Terra Nova, 15*, 109–117.

Burg, J. P., Kaus, B. J. P., & Podladchikov, Y. Y. (2004). Dome structures in collision orogens: Mechanical investigation of the gravity/compression interplay.

In D. L. Whitney, et al. (Eds.), *Gneiss domes in orogeny, special paper* (pp. 47–66). Boulder: Geological Society of America.
Butler, J. P., Beaumont, C., & Jamieson, R. A. (2013). The Alps 1: A working geodynamic model for burial and exhumation of (ultra) high-pressure rocks in Alpine-type orogens. *Earth and Planetary Science Letters, 377*, 114–131.
Butler, R. W. H., & Freeman, S. (1996). Can crustal extension be distinguished from thrusting in the internal parts of mountain belts? A case history of the Entrelor shear zone, Western Alps. *Journal of Structural Geology, 18*(7), 909–923.
Cadoppi, P., Castelletto, M., Sacchi, R., Baggio, P., Carraro, F., & Giraud, V. (2002). Note illustrative della Carta Geologica d'Italia alla scala 1:50.000 – Foglio 154, Susa. *Servizio Geologico d'Italia*, p. 127.
Cartwright, I., & Barnicoat, A. C. (2002). Petrology, geochronology, and tectonics of shear zones in the Zermatt-Saas and Combin zones of the Western Alps. *Journal of Metamorphic Geology, 20*, 263–281.
Dal Piaz, G. V., Bistacchi, A., & Massironi, M. (2003). Geological outline of the Alps. *Episodes, 26*(3), 175–180.
Dal Piaz, G., Cortiana, G., Del Moro, A., Martin, S., Pennacchioni, G., & Tartarotti, P. (2001). Tertiary age and paleostructural inferences of the eclogitic imprint in the Austroalpine outliers and Zermatt-Saas ophiolite, Western Alps. *International Journal of Earth Sciences, 90*(3), 668–684.
Deville, E., Fudral, S., Lagabrielle, Y., Marthaler, M., & Sartori, M. (1992). From oceanic closure to continental collision: A synthesis of the "schistes lustrés" metamorphic complex of the Western Alps. *Geological Society of America Bulletin, 104*, 127–139.
Festa, A., Balestro, G., Borghi, A., De Caroli, S., & Succo, A. (2020). The role of structural inheritance in continental break-up and exhumation of Alpine Tethyan mantle (Canavese Zone, Western Alps). *Geoscience Frontiers, 11*(1), 167–188.
Festa, A., Pini, G. A., Ogata, K., & Dilek, Y. (2019). Diagnostic features and field-criteria in recognition of tectonic, sedimentary and diapiric mélanges in orogenic belts and exhumed subduction-accretion complexes. *Gondwana Research, 74*, 7–30.
Freeman, S. R., Inger, S., Butler, R. W. H., & Cliff, R. A. (1997). Dating deformation using Rb–Sr in white mica: Greenschist-facies deformation ages from the Entrelor shear Zone, Italian Alps. *Tectonics, 16*, 57–76.
Froitzheim, N., Pleuger, J., & Nagel, T. J. (2006). Extraction faults. *Journal of Structural Geology., 28*(8), 1388–1395.
Ganne, J., Bertrand, J., Fudral, S., Marquer, D., & Vidal, M. (2007). Structural and metamorphic evolution of the Ambin massif (Western Alps). *Bulletin de la Société géologique de France, 178*, 437–458.
Ganne, J., Bussy, F., & Vidal, O. (2003). Multi-stage garnet in the internal Brianconnais basements (Ambin and South Vanoise massifs): New petrological constraints on the blueschist-facies metamorphism in the Western Alps and tectonic implications. *Journal of Petrology, 44*, 1281–1308.
Ganne, J., Marquer, D., Rosenbaum, G., Bertrand, J., & Fudral, S. (2006). Partitioning of deformation within a subduction channel during exhumation of high-pressure rocks: A case study from the Western Alps. *Journal of Structural Geology, 28*, 1193–1207.
Gasco, I., Gattiglio, M., & Borghi, A. (2009). Structural evolution of different tectonic units across the Austroalpine-Penninic boundary in the middle Orco Valley (Western Italian Alps). *Journal of Structural Geology, 31*, 301–314.
Gasco, I., Gattiglio, M., & Borghi, A. (2011). Lithostratigraphic setting and P-T metamorphic evolution for the Dora Maira Massif along the Piedmont Zone boundary (middle Susa Valley, NW Alps). *International Journal of Earth Sciences, 100*, 1065–1085.
Gasco, I., Gattiglio, M., & Borghi, A. (2013). Review of metamorphic and kinematic data from Internal Crystalline Massifs (Western Alps): PTt paths and exhumation history. *Journal of Geodynamics, 63*, 1–19.
Gauthiez-Putallaz, L., Rubatto, D., & Hermann, J. (2016). Dating prograde fluid pulses during subduction by in situ U-Pb and oxygen isotope analysis. *Contributions to Mineralogy and Petrology, 171*, 1–20.
Ghignone, S., & Gattiglio, M. (2013). Late to post-metamorphic cross-section trough the Piedmont Zone in the lower Susa Valley (Western Alps). *Rendiconti OnLine della Società Geologica Italiana, 29*, 66–69.
Ghignone, S., Gattiglio, M., Balestro, G., & Borghi, A. (2020a). Geology of the Susa Shear Zone (Susa Valley, Western Alps). *Journal of Maps, 16*(2), 79–86. https://doi.org/10.1080/17445647.2019.1698473.
Ghignone, S., Borghi, A., Balestro, G., Castelli, D., Gattiglio, M., & Groppo, C. (2020b). HP-tectono-metamorphic evolution of the Internal Piedmont Zone in Susa Valley (Western Alps): New petrologic insight from garnet+chloritoid –bearing micaschists and Fe-Ti metagabbro. *Journal of Metamorphic Geology*. https://doi.org/10.1111/JMG.12574.
Goscombe, B. D., & Passchier, C. W. (2003). Asymmetric boudins as shear sense indicators—an assesment from field data. *Journal of Structural Geology, 25*(4), 575–589.
Groppo, C., & Castelli, D. (2010). Prograde P-T evolution of a lawsonite eclogite from the Monviso meta-ophiolite (Western Alps): Dehydration and redox reactions during subduction of oceanic FeTi-oxide gabbro. *Journal of Petrology, 51*, 2489–2514.
Kirst, F., & Leiss, B. (2017). Kinematics of syn- and post-exhumational shear zones at Lago di Cignana (Western Alps, Italy): Constraints on the exhumation of Zermatt-Saas (ultra)high-pressure rocks and deformation along the Combin fault and Dent Blanche Basal Thrust. *International Journal of Earth Science, 106*(1), 215–236.
Kurz, W., & Froitzheim, N. (2002). The exumation of eclogite facies metamorphic rocks—a review of models confronted with models from the Alps. *International Geological Review, 44*(8), 702–743.
Lardeaux, J., Schwartz, S., Tricart, P., Paul, A., Guillot, S., Béthoux, N., et al. (2006). A crustal-scale crosssection of the south-western Alps combining geophysical and geological imagery. *Terra Nova, 18*(6), 412–422.
Le Bayon, B., & Ballèvre, M. (2006). Deformation history of a subducted continental crust (Gran Paradiso, Western Alps): Continuing crustal shortening during exhumation. *Journal of Structural Geology, 28*(5), 793–815.
Leardi, L., & Rossetti, P. (1985). Caratteri geologici e petrografici delle metaofioliti della Val d'Ala (valli di Lanzo, Alpi Graie). *Bollettino dell'Associazione Mineraria Subalpina, 22*, 421–441.
Lemoine, M., & Tricart, P. (1986). Les Schistes lustrés des Alpes occidentales: Approche stratigraphique, structurale et sedimentologique. *Eclogae Geologicae Helvetiae, 79*, 271–294.
Lorenzoni, S. (1968). Etude pétrographique du versant italien du massif d'Ambin (Alpes franco italiennes). *Schweizerische Mineralogische und Petrologische Mitteilungen, 48*(1), 428–436.
Malusà, M. G., Polino, R., & Martin, S. (2005). The Gran San Bernardo nappe in the Aosta valley (Western Alps): A composite stack of distinct continental crust units. *Bulletin de la Societe Geologique de France, 176*(5), 417–431.
Manzotti, P., Ballèvre, M., Zucali, M., Robyr, M., & Engi, M. (2014). The tectono-metamorphic evolution of the Sesia-Dent Blanche nappes (internal Western Alps): Review and synthesis. *Swiss Journal of Geosciences, 107*, 309–336.
Manzotti, P., Bosse, V., Pitra, P., Robyr, M., Schiavi, F., & Ballèvre, M. (2018). Exhumation rates in the Gran Paradiso Massif (Western Alps) constrained by in situ U-Th–Pb dating of accessory phases (monazite, allanite and xenotime). *Contributions to Mineralogy and Petrology, 173*(3), 24.
Marthaler, M., Fudral, S., Deville, E., & Rampnoux, J. P. (1986). Mise en évidence du Crétacé supérieur dans la couverture septentrionale de Dora-Maira, région de Suse, Italie (Alpes Occidentales). Conséquences paléogéographyques et structurales. *Comptes Rendus de l'Académie des Sciences Paris, 302*(2), 91–96.
Martin, S., Tartarotti, P., & Dal Piaz, G. V. (1994). The Mesozoic ophiolites of the Alps: A review. *Bollettino di Geofisica Teorica e Applicata, 36*, 175–219.
Michard, A., Avigad, D., Goffé, B., & Chopin, C. (2003). The high-pressure metamorphic front of the south Western Alps (Ubaye-Maira transect, France, Italy). *Schweizerische Mineralogische und Petrographische Mitteilungen, 84*, 215–235.
Michard, A., Goffe, B., Chopin, C., & Henry, C. (1996). Did the Western Alps develop through an Oman-type stage? The geotectonic setting of high-pressure metamorphism in two contrasting Tethyan transects. *Eclogae Geologicae Helvetiae, 89*, 43–80.
Michel, R. (1953). Les Schistes cristallins du massif du Grand Paradis et de Sesia-Lanzo (Alpes franco-italiennes). *Sciences de la Terre, Nancy*, pp. 1–287.
Mies, J. W. (1993). Structural analysis of sheath folds in the Sylacauga Marble Group, Talladega slate belt, southern Appalachians. *Journal of Structural Geology, 15*, 983–993.
Negro, F., Bousquet, R., Vils, F., Pellet, C.-M., & Hänggi-Schaub, J. (2013). Thermal structure and metamorphic evolution of the Piemont-Ligurian metasediments in the northern Western Alps. *Swiss Journal of Geosciences, 106*, 63–78.
Nicolas, A. (1966). Étude pétrochimique des Roches vertes et de leurs minéraux entre Dora Maira et Grand Paradis (Alpes piémontaises); le complexe

ophiolite-schistes lustrés. *Ph.D. dissertation, University of Nantes, France,* p. 299.
Perrone, G., Eva, E., Solarino, S., Cadoppi, P., Balestro, G., Fioraso, G., et al. (2010). Seismotectonic investigations in the inner Cottian Alps (Italian Western Alps): An integrated approach. *Tectonophysics, 496*(1–4), 1–16.
Philippot, P. (1990). Opposite vergence of nappes and crustal extension in the French-Italian Western Alps. *Tectonics, 9*(5), 1143–1164.
Platt, J. P. (1993). Exhumation of high-pressure rocks: A review of concept and processes. *Terra Nova, 5*(2), 119–133.
Platt, J. P., & Vissers, R. L. M. (1980). Extensional structures in anisotropic rocks. *Journal of Structural Geology, 2*(4), 397–410.
Pleuger, J., Roller, S., Walter, J. M., Jansen, E., & Froitzheim, N. (2007). Structural evolution of the contact between two Penninic nappes (Zermatt-Saas zone and Combin zone, Western Alps) and implications for the exhumation mechanism and palaeogeography. *International Journal of Earth Sciences, 96*(2), 229–252.
Pognante, U. (1979). The Orsiera-Rocciavrè metaophiolitic complex (Italian Western Alps). *Ofioliti, 4*(2), 183–198.
Pognante, U. (1983). Les intercalations gneissiques dans une unite des "schistes lustrés" de la valleé de Suse (Alpes Occidentales): Témoins d'une marge continentale subductée? *Comptes Rendus de l'Académie des Sciences Paris, 296*(2), 379–382.
Polino, R., Dela Pierre, F., Borghi, A., Carraro, F., Fioraso, G., & Giardino, M. (2002). Note illustrative della Carta Geologica d'Italia alla scala 1:50.000 - Foglio 153 Bardonecchia. *Servizio Geologico d'Italia,* p. 128.
Reddy, S. M., Wheeler, J., Butler, R. W. H., Cliff, R. A., Freeman, S., Inger, S., et al. (2003). Kinematic reworking and exhumation within the convergent Alpine Orogen. *Tectonophysics, 365*(1–4), 77–102.
Reddy, S. M., Wheeler, J., & Cliff, R. A. (1999). The geometry and timing of orogenic extension: An example from the Western Italian Alps. *Journal of Metamorphic Geology, 17*(5), 573–589.
Ricou, L. E., & Siddans, W. B. (1986). Collision tectonics in the Western Alps. In M. P. Coward & A. C. Ries (Eds.), *Collision tectonics, special publication* (pp. 229–244). London: Geological Society of London.
Ring, U. (1995). Horizontal contraction or horizontal extension? Heterogeneous Late Eocene and Early Oligocene general shearing during blueschist and greenschist facies metamorphism at the Pennine-Austroalpine boundary zone in the Western Alps. *Geologische Rundschau, 84*, 843–859.
Rolland, Y., Lardeaux, J. M., Guillot, S., & Nicollet, C. (2000). Extension syn-convergence, poinçonnement vertical et unités metamorphiques contrastées en bordure ouest du Gran Paradis (Alpes Franco-Italiennes). *Geodinamica Acta, 13*, 133–148.
Rosenbaum, G., & Lister, G. S. (2005). The Western Alps from the Jurassic to Oligocene: Spatio-temporal constraints and evolutionary reconstructions. *Earth Science Reviews, 69*(3–4), 281–306.
Rosenbaum, G., Menegon, L., Glodny, J., Vasconcelos, P., Ring, U., Massironi, M., et al. (2012). Dating deformation in the Gran Paradiso Massif (NW Italian Alps): Implications for the exhumation of high-pressure rocks in a collisional belt. *Lithos, 144–145*, 130–144.
Sandrone, R., Cadoppi, P., Sacchi, R., & Vialon, P. (1993). The Dora-Maira massif. In J. F. von Raumer & F. Neubauer (Eds.), *Pre-Mesozoic Geology in the Alps* (pp. 317–325). Berlin: Springer.
Savignano, E., Reddy, S. M., Bridges, J., & Mazzoli, S. (2016). Quartz fabric variations across the greenschist facies shear zone separating the Zermatt-Saas and combin ophiolitic zones, Upper Val Gressoney, Western Alps. *Ofioliti, 41*, 85–98.
Schmid, S. M., & Kissling, E. (2000). The arc of the Western Alps in the light of geophysical data on deep crustal structure. *Tectonics, 19*, 62–85.
Schmid, S. M., Kissling, E., Diehl, T., van Hinsbergen, D. J. J., & Molli, G. (2017). Ivrea mantle wedge, arc of the Western Alps, and kinematic evolution of the Alps-Apennines orogenic system. *Swiss Journal of Geosciences., 110*(2), 581–612.
Schwartz, S., Tricart, P., Lardeaux, J. M., Guillot, S., & Vidal, O. (2009). Late tectonic and metamorphic evolution of the Piedmont accretionary wedge (Queyras Schistes lustrés, Western Alps): Evidences for tilting during Alpine collision. *Geological Society of America Bulletin, 121*, 502–518.
Strzerzynski, P., Guillot, S., Leloup, P. H., Arnaud, N., Vidal, O., Ledru, P., et al. (2012). Tectono-metamorphic evolution of the Briançonnais zone (Modane-Aussois and Southern Vanoise units, Lyon Turin transect, Western Alps). *Eclogae Geologicae Helvetiae, 56–57*, 55–75.
Tartarotti, P., Festa, A., Benciolini, L., & Balestro, G. (2017). Record of Jurassic mass transport processes through the orogenic cycle: Understanding chaotic rock units in the high-pressure Zermatt-Saas ophiolite (Western Alps). *Lithosphere, 9*(3), 399–407.
Tricart, P., & Schwartz, S. (2006). A north-south section across the Queyras Schistes lustre´s (Piedmont zone, Western Alps): Syn-collision refolding of a subduction wedge. *Eclogae Geologicae Helvetiae, 99*, 429–442.
Tricart, P., Schwartz, S., Sue, C., & Lardeaux, J. M. (2004). Evidence of synextension tilting and doming during final exhumation from analysis of multi-stage faults (Queyras Schistes lustrés, Western Alps). *Journal of Structural Geology, 26*(9), 1633–1645.
Vialon, P. (1966). Étude géologique du massif cristallin Dora-Maira, Alpes cottiennes internes, Italie. *Travaux du Laboratoire de Géologie de Grenoble, Mèmoires., 4*, 282.
Vissers, R. L. M., Van Hinsbergen, D. J. J., Meijer, P. T. H., & Piccardo, G. B. (2013). Kinematics of Jurassic ultraslow spreading in the Piemonte Ligurian ocean. *Earth and Planetary Science Letters, 380*, 138–150.
Wang, K., Burov, E., Gumiaux, C., Chen, Y., Lu, G., Mezri, L., et al. (2015). Formation of metamorphic core complexes in non-over-thickened continental crust: A case study of Liaodong Peninsula (East Asia). *Lithos, 238*, 86–100.
Weber, S., Sandmann, S., Miladinova, I., Fonseca, R. O. C., Froitzheim, N., Münker, C., et al. (2015). Dating the initiation of Piemonte-Liguria Ocean subduction: Lu–Hf garnet chronometry of eclogites from the Theodul Glacier Unit (Zermatt-Saas zone, Switzerland). *Swiss Journal of Geosciences, 108*(2–3), 183–199.
Wheeler, J., & Butler, R. W. H. (1993). Evidence for extension in the western Alpine orogen: The contact between the oceanic Piemonte and overlying continental Sesia units. *Earth and Planetary Science Letters, 117*, 457–474.
Wheeler, J., Reddy, S. M., & Cliff, R. A. (2001). Kinematic linkage between internal zone extension and shortening in more external units in the NW Alps. *Journal of the Geological Society of London, 158*(3), 439–443.

Publisher's Note